

## Accelerating Unimolecular Decarboxylation by Preassociated Acid Catalysis in Thiamin-Derived Intermediates: Implicating Brønsted Acids as Carbanion Traps in Enzymes

Ronald Kluger,\* Glenn Ikeda, Qingyan Hu, Pengpeng Cao, and Joel Drewry

Contribution from the Davenport Chemical Research Laboratories, Department of Chemistry,  
University of Toronto, Toronto, Ontario, Canada M5S 3H6

Received August 28, 2006; E-mail: rkluger@chem.utoronto.ca

**Abstract:** Mandelylthiamin (MT) is formally the conjugate of thiamin and benzoylformate. It is the simplified analogue of the first covalent intermediate in benzoylformate decarboxylase. Although MT is the functional equivalent of the enzymic intermediate, it is  $10^6$ -fold less reactive in decarboxylation. Furthermore, upon loss of carbon dioxide, it undergoes a fragmentation reaction that is about  $10^2$ -fold faster than the enzymic reaction. While Brønsted acids in general can suppress the fragmentation to some extent, they do not accelerate the decarboxylation. Surprisingly, the conjugate acid of pyridine accelerates decarboxylation; it also blocks fragmentation with particularly high efficiency. These results are consistent with the conjugate acid of pyridine acting as a "spectator" catalyst, associating with MT prior to decarboxylation. In the absence of catalyst, carbon dioxide formed upon carbon–carbon bond breaking overwhelmingly reverts to the carboxylate. Association of pyridine (and its conjugate acid) with MT permits trapping of the nascent carbanion by protonation, while nonassociated acids must arrive by the relatively slow process of diffusion. C-Alkyl pyridine acids provide similar catalysis while other acids have no effect. This suggests that an enzyme that generates an aldehyde from a 2-ketoacid should have functional Brønsted acids in their active sites that would trap the carbanion, as does benzoylformate decarboxylase. Enzymes that give nonaldehydic products from decarboxylation of thiamin diphosphate conjugates containing an associated electron acceptor or electrophilic substrate would also be able to prevent the reversal of decarboxylation.

### Introduction

Thiamin diphosphate (TDP)-dependent enzymes catalyze reactions through protein-bound covalent intermediates derived from the substrate and cofactor.<sup>1</sup> The reactivity of synthesized conjugates of thiamin that parallel these intermediates provides a quantitative basis for evaluating the specific role of proteins in the enzymic reactions as well as giving insights into the detailed mechanism associated with the cofactor.<sup>2,3</sup> Recent spectroscopic and crystallographic studies have shown that these intermediates can even be observed and quantified on the enzymes.<sup>4–10</sup>

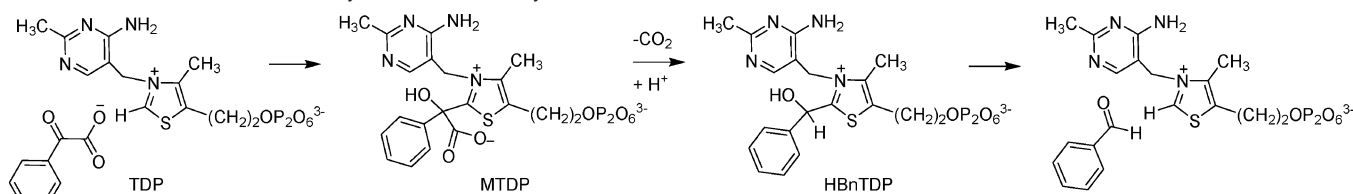
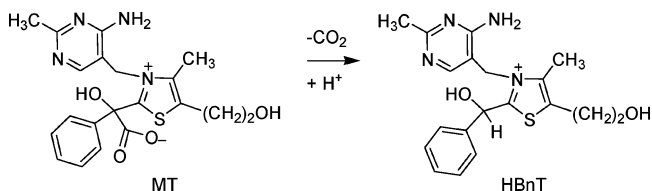
Based on these considerations, we have been investigating the reactivity of intermediates in the conversion of benzoyl-

formate to benzaldehyde and carbon dioxide. The enzymatic reaction superficially resembles the decarboxylation of pyruvate. It is specifically catalyzed by benzoylformate decarboxylase (BFD).<sup>11–17</sup> The enzyme avoids formation of a benzoyl anion by addition of enzyme-bound thiamin diphosphate (TDP) to the carbonyl group of benzoylformate, producing enzyme-bound 2-(2-mandelyl)TDP (MTDP, Scheme 1). Loss of carbon dioxide from MTDP, followed by protonation of the resulting carbanion equivalent, yields the precursor of benzaldehyde, 2-(1-hydroxybenzyl)TDP (HBnTDP). Breakdown of HBnTDP, via initial formation of its C2 $\alpha$ -alkoxide, releases benzaldehyde and TDP.

The key covalent intermediate, MTDP, appears to be set up electronically for substitution of a proton for carbon dioxide via an enamine intermediate (from delocalization of the adjacent

- (1) Kluger, R. *Chem. Rev.* **1987**, 87, 863–876.
- (2) Alvarez, F. J.; Ermer, J.; Huebner, G.; Schellenberger, A.; Schowen, R. L. *J. Am. Chem. Soc.* **1991**, 113, 8402–9.
- (3) Schowen, R. L. In *Comprehensive Biological Catalysis*; Sinnott, M. L., Ed.; Academic Press: London, 1998; Vol. 2, pp 217–266.
- (4) Wille, G.; Meyer, D.; Steinmetz, A.; Hinze, E.; Golbik, R.; Tittmann, K. *Nat. Chem. Biol.* **2006**, 2, 324–328.
- (5) Tittmann, K. *Bioforum* **2005**, 28, 44–46.
- (6) Schütz, A.; Golbik, R.; König, S.; Hübner, G.; Tittmann, K. *Biochemistry* **2005**, 44, 6164–6179.
- (7) Tittmann, K.; Golbik, R.; Uhlemann, K.; Khailova, L.; Schneider, G.; Patel, M.; Jordan, F.; Chipman, D. M.; Duggleby, R. G.; Huebner, G. *Biochemistry* **2003**, 42, 7885–7891.
- (8) Arjunan, P.; Sax, M.; Brunskill, A.; Chandrasekhar, K.; Nemeria, N.; Zhang, S.; Jordan, F.; Furey, W. *J. Biol. Chem.* **2006**, 281, 15296–15303.
- (9) Jordan, F.; Nemeria, N. S. *Bioorg. Chem.* **2005**, 33, 190–215.
- (10) Zhang, S.; Liu, M.; Yan, Y.; Zhang, Z.; Jordan, F. *J. Biol. Chem.* **2004**, 279, 54312–54318.

- (11) Reynolds, L. J.; Garcia, G. A.; Kozarich, J. W.; Kenyon, G. L. *Biochemistry* **1988**, 27, 2217–2212.
- (12) Hasson, M. In *Thiamin Pyrophosphate Biochemistry*; Bisswanger, H., Schellenberger, A., Eds.; Blaubeuren, Germany, 1996.
- (13) Hasson, M. S.; Muscate, A.; Henehan, G. T.; Guidinger, P. F.; Petsko, G. A.; Ringe, D.; Kenyon, G. L. *Protein Sci.* **1995**, 4, 955–9.
- (14) Hasson, M. S.; Muscate, A.; McLeish, M. J.; Polovnikova, L. S.; Gerlt, J. A.; Kenyon, G. L.; Petsko, G. A.; Ringe, D. *Biochemistry* **1998**, 37, 9918–9930.
- (15) Reynolds, L. J.; Garcia, G. A.; Kozarich, J. W.; Kenyon, G. L. *Biochemistry* **1988**, 27, 5530–8.
- (16) Weiss, P. M.; Garcia, G. A.; Kenyon, G. L.; Cleland, W. W.; Cook, P. F. *Biochemistry* **1988**, 27, 2197–205.
- (17) Polovnikova, E. S.; McLeish, M. J.; Sergienko, E. A.; Burgner, J. T.; Anderson, N. L.; Bera, A. K.; Jordan, F.; Kenyon, G. L.; Hasson, M. S. *Biochemistry* **2003**, 42, 1820–30.

**Scheme 1.** Intermediates in Benzoylformate Decarboxylase**Scheme 2.** Decarboxylation of MT; the Conjugate of Thiamin and Benzoylformate

thiazolium ring). The diphosphate side chain of TDP is not involved in catalysis but does bind the cofactor to the protein through coordination to a magnesium ion, allowing precise positioning in the active site.<sup>14,17</sup> The simplified but chemically correct analogue of MTDP, 2-(2-mandelyl)thiamin (MT), the conjugate of benzoylformate and thiamin, undergoes decarboxylation at a relatively rapid rate compared to most carboxylic acids (Scheme 2).<sup>18</sup>

Yet, the rate constants for the decarboxylation of MT are much smaller than that for the comparable enzymic reaction:  $k_{\text{cat}}$  for BFD exceeds the unimolecular decarboxylation rate constant of MT by a factor of about  $10^6$ . Another critical point of divergence is the observation that the product of decarboxylation of MT, the conjugate base of 2-(1-hydroxybenzyl)thiamin (HBN), undergoes a fast fragmentation reaction that cleaves the thiamin-derived portion of the conjugate base of HBN. The rate constant for fragmentation is about  $10^2$  times larger than the enzymic  $k_{\text{cat}}$  (Scheme 3). Protonation of the HBN carbanion at C2 $\alpha$  competes with fragmentation and produces HBNH.<sup>19</sup> Thus, the protein accelerates the decarboxylation step while reducing the rate of the fragmentation process. The extent to which the fragmentation process occurs provides a measure or “clock” versus the protonation reaction that produces HBNH. In this paper we present evidence for a previously undetected form of acid catalysis in decarboxylation that was the subject of a preliminary report.<sup>20</sup> This mechanism provides a basis for explaining the enigmatic distinctions of the enzymic and nonenzymic reactions of the intermediates. It also provides more general insights into how decarboxylation may be catalyzed in other systems.

## Experimental Section

**Materials and Methods. Spectra.** <sup>1</sup>H NMR spectra were recorded at 400 MHz in deuterium oxide. Chemical shifts are relative to DSS (2,2-dimethyl-2-silapentane-5-sulfonate sodium salt). <sup>13</sup>C NMR spectra were recorded at 100 MHz in deuterium oxide with chemical shifts relative to DSS. IR: FT spectra were recorded with samples in KBr pellets. Mass spectra were recorded on an ESI instrument at medium resolution.

**Synthesis of MT.** Thiamin chloride hydrochloride (5.0 g, 0.015 mol) was suspended in 80 mL of ethanol. The mixture was purged with

argon and cooled to  $-5^\circ\text{C}$ . A solution of ethyl benzoylformate (8.2 mL, 3.5 equiv) and anhydrous magnesium chloride (0.6 g, 0.4 equiv) in 50 mL of ethanol was deoxygenated and immediately added under nitrogen to the thiamin solution. A sodium ethoxide solution (0.7 g of sodium in 40 mL of ethanol) was deoxygenated and added to the mixture with stirring. After 10 min at  $-5^\circ\text{C}$ , the solution was acidified with 12 M hydrochloric acid. The precipitate, consisting of sodium chloride and unreacted thiamin, was removed by filtration. The filtrate was concentrated by rotary evaporation at  $25^\circ\text{C}$  to a minimal volume, which was then dissolved in 25 mL of water and washed with  $3 \times 50$  mL portions of dichloromethane. The aqueous layer was stirred with Chelex resin (sodium form) for 1–2 h at pH 6 to remove magnesium. After filtration, the aqueous solution was acidified and lyophilized to dryness. The resulting yellow solid was dissolved in ethanol, filtered, and eluted on cellulose with 1:4 (v/v) ethanol/ethyl acetate to give 0.33 g (5%) of the ethyl ester of MT (attempts to increase this amount have not yet been successful).

<sup>1</sup>H NMR (400 MHz, DCl in D<sub>2</sub>O relative to internal DSS):  $\delta$  1.30 (3H, t,  $J = 7.2$  Hz,  $\text{CH}_3\text{CH}_2\text{OCO}$ ), 2.41 (3H, s,  $\text{CH}_3\text{—C2'}$  pyrimidine), 2.49 (3H, s,  $\text{CH}_3\text{—thiazole}$ ), 3.25 (2H, t,  $J = 5.8$  Hz,  $\text{CH}_2\text{CH}_2\text{OH}$ ), 3.94 (2H, t,  $J = 5.8$  Hz,  $\text{CH}_2\text{CH}_2\text{OH}$ ), 4.43 (2H, q,  $J = 7.2$  Hz,  $\text{CH}_2\text{CH}_2\text{OCO}$ ), 5.36 (1H, d,  $J = 18$  Hz,  $\text{H}_a\text{H}_b\text{CN}$ ), 5.86 (1H, d,  $J = 18$  Hz,  $\text{H}_a\text{H}_b\text{CN}$ ), 6.81 (1H, s,  $\text{H—C6'}$  pyrimidine), 7.32 (3H, m, aromatic), 7.54 (2H, m, aromatic). <sup>13</sup>C NMR (100 MHz, DCl in D<sub>2</sub>O relative to internal DSS):  $\delta$  194.53, 169.71, 161.74, 160.85, 145.57, 137.99, 136.25, 135.15, 130.07, 129.92, 126.14, 107.55, 65.72, 60.36, 49.38, 47.49, 29.63, 20.94, 13.39, 11.90. IR: 3390 (broad), 1631. ESIMS of parent peak  $[\text{C}_{22}\text{H}_{27}\text{N}_4\text{O}_4\text{S}]^+$ , calcd 443, found 443.

The ethyl ester was hydrolyzed in concentrated hydrochloric acid for 6 days at room temperature. After concentration under a vacuum and lyophilization, the chloride hydrochloride salt of MT was obtained (stored dry at  $-20^\circ\text{C}$ ).

<sup>1</sup>H NMR (400 MHz, DCl in D<sub>2</sub>O relative to internal DSS):  $\delta$  2.39 (3H, s,  $\text{CH}_3\text{—C2'}$  pyrimidine), 2.49 (3H, s,  $\text{CH}_3\text{—thiazole}$ ), 3.23 (2H, t,  $J = 5.8$  Hz,  $\text{CH}_2\text{CH}_2\text{OH}$ ), 3.94 (2H, t,  $J = 5.8$  Hz,  $\text{CH}_2\text{CH}_2\text{OH}$ ), 5.41 (1H, d,  $J = 18$  Hz,  $\text{H}_a\text{H}_b\text{CN}$ ), 5.90 (1H, d,  $J = 18$  Hz,  $\text{H}_a\text{H}_b\text{CN}$ ), 6.82 (1H, s,  $\text{H—C6'}$  pyrimidine), 7.30 (3H, m, aromatic), 7.55 (2H, m, aromatic). ESIMS  $[\text{C}_{20}\text{H}_{23}\text{N}_4\text{O}_4\text{S}]^+$ , calcd 415, found 371 (MT loses  $\text{CO}_2$  upon ionization, calcd 371).

**Kinetics.** Measurements of the rate of decarboxylation of MT were conducted using buffer solutions maintained at  $25.0^\circ\text{C}$  in a jacketed beaker with a circulating water bath. In solutions whose acidity was  $\text{pH} < 4.0$ , the reaction was followed at 295 nm. Between pH 4.5 and 8.5, the decarboxylation was followed at 328 nm (the absorbance of a fragmentation product, PTK, see below). Under these conditions the reactions gave an isosbestic point. Above pH 8.5, no isosbestic point was observed. <sup>1</sup>H NMR analysis indicated that the ring-opened derivative of thiamin (from addition of hydroxide)<sup>21</sup> and benzoylformate are the principal products (decarboxylation is not base catalyzed so that it becomes insignificant in these solutions; see Figure 1). Under these conditions, thiamin undergoes ring opening at a rapid rate, comparable to the rate of elimination of benzoylformate from MT. The two processes were followed at 248 nm and 274 nm, and the rate constants were obtained using a multiwavelength algorithm.<sup>22</sup>

(18) Hu, Q.; Kluger, R. *J. Am. Chem. Soc.* **2002**, *124*, 14858–14859.

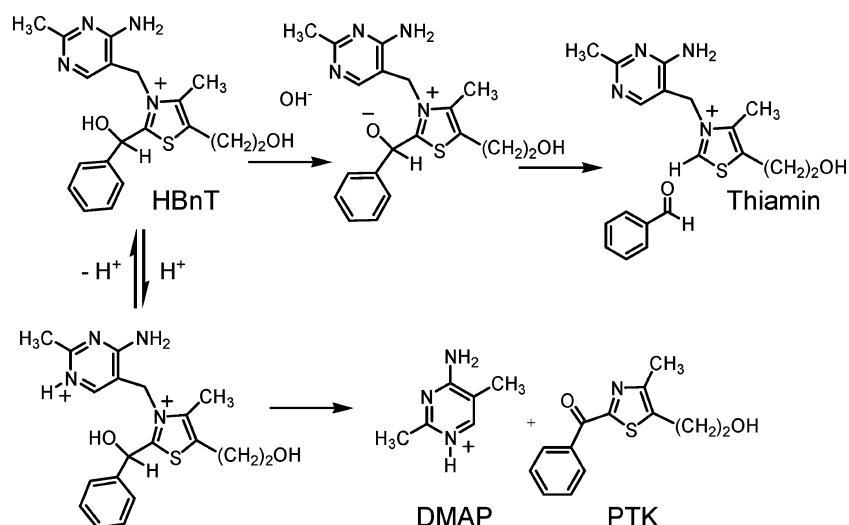
(19) Hu, Q.; Kluger, R. *J. Am. Chem. Soc.* **2004**, *126*, 68–69.

(20) Hu, Q.; Kluger, R. *J. Am. Chem. Soc.* **2005**, *127*, 12242–12243.

(21) Maier, G. D.; Metzler, D. E. *J. Am. Chem. Soc.* **1957**, *79*, 4386–4391.

(22) Kluger, R.; Chin, J.; Smyth, T. *J. Am. Chem. Soc.* **1981**, *103*, 884–8.

Scheme 3. Competing Routes from HBnT



Reactions that were followed at 328 nm tracked one of the fragmentation products (phenyl thiazole ketone, PTK;  $\epsilon = 10\,000$ ). This forms rapidly after the slow conversion of MT to the conjugate base of HBnT by loss of carbon dioxide. Ionic strength was maintained at 1.0 with potassium chloride. The dependence of rate on buffer concentration for each buffer was determined at  $\text{pH} = \text{p}K_a'$ . For the evaluation of the effects of ethanol and *N*-ethylpyridinium, 0.2 M pyridine was used to maintain  $\text{pH} = \text{p}K_a' = 5.4$ . Data were collected with an interfaced computer. Observed first-order rate constants were calculated from nonlinear regression fitting of the data to the integrated first-order rate expression. Apparent second-order rate constants were obtained from the slopes of plots of the observed first-order rate constants as a function of buffer concentration.

**Product Analysis.** PTK and DMAP are formed along with HBnT during the decarboxylation of MT. The HBnT formed initially eventually fragments (via regeneration of its C2 $\alpha$  conjugate base) to PTK and DMAP.<sup>19,23</sup> The relative concentrations of initially formed PTK and HBnT were obtained by extrapolation of the absorbance at 328 nm to the start and end of the reaction. The total amount of PTK and HBnT formed initially is obtained from the absorbance at 328 nm after HBnT is converted to PTK by incubation at 60 °C for 1 week in

combination with initially formed PTK. The resulting solutions give the final absorbance at 328 nm ( $\text{abs}_f$ ). The fraction of MT converted to HBnT upon decarboxylation is the difference of the ratios of the absorbance at 328 nm (PTK) after the initial reaction and  $\text{abs}_f$  divided by  $\text{abs}_f$  corrected for the initial absorbance.

$$\% \frac{\text{HBnT}}{\text{total}} = \frac{\text{abs}_f - \text{abs}_i}{\text{abs}_f - \text{abs}_0} \times 100\% \quad (1)$$

**Molecular Orbital Calculations.** Geometry optimization of MT was performed based on the crystal structure of HBnT reported by Hu and co-workers<sup>24</sup> with Spartan software using the semiempirical PM3 method.

## Results

The synthesis of the addition product from benzoylformate and thiamin, 2-(2-mandelyl)thiamin (MT), was achieved by condensation of the C2-conjugate base of thiamin (from thiamin and sodium ethoxide) with ethyl benzoylformate in ethanol in the presence of magnesium chloride. Hydrolysis of the ester in concentrated acid occurs without decarboxylation of the product. For comparison, the synthesis of the less-hindered  $\alpha$ -lactylthiamin (via ethyl pyruvate and thiamin) occurs without the need for addition of magnesium chloride and in much higher yield.<sup>22</sup> The bulk and electronic stabilization of ethyl benzoylformate are likely to make the addition less favorable. We assume that chelation of the magnesium ion by benzoylformate promotes the addition reaction.

The pH–rate profile and product distribution for the decarboxylation of MT provide a quantitative basis for comparison with the enzymic reaction that occurs via protein-bound MTDP. MT is sufficiently stable to be isolated and purified if its carboxyl group is maintained in the acid form. The pH–rate profile for the reactions of MT is shown in Figure 1.

The profile shows distinct features that relate to the structure and reactions of MT. The loss of carbon dioxide requires that the carboxyl group is not protonated, hence the increase from the highly acid region toward 0.01 M acid, leveling at pH 3.

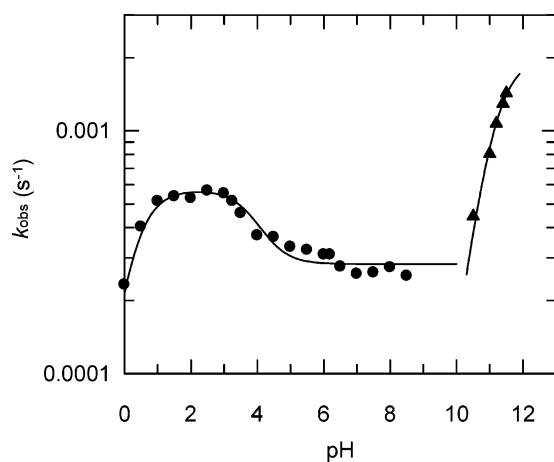
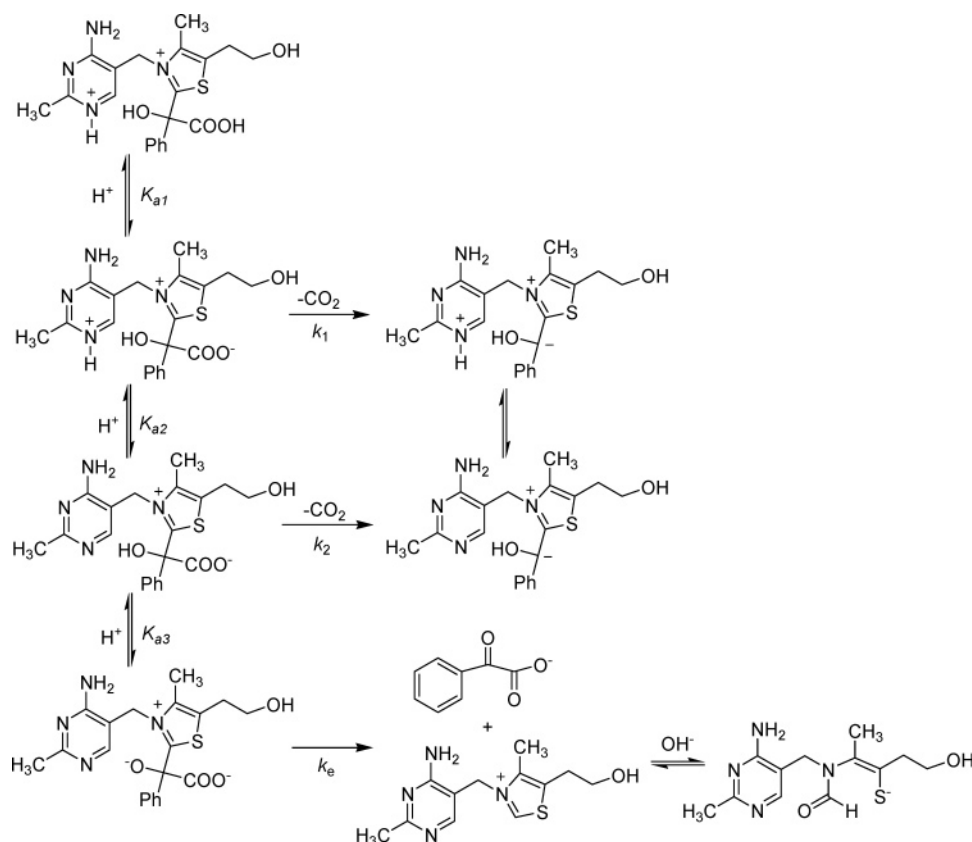


**Figure 1.** Observed first-order rate constants for decarboxylation of MT (●) and elimination of benzoylformate from MT (▲) as a function of pH or  $-\log[\text{acid}]$ . The data were fit to eq 2 for the decarboxylation reaction (below pH 9) and eq 3 (above pH 10) for the elimination reaction (Scheme 4 summarizes the complex set of competing and parallel reactions). Parameters generated in fitting the curve:  $K_{a1} = 0.6$ ,  $K_{a2} = 1.2 \times 10^{-4}$  (dissociation of the di- and monoacids of MT) in eq 1 as well as the rate constants presented later.

(23) Kluger, R.; Moore, I. F. *J. Am. Chem. Soc.* **2000**, *122*, 6145–6150.

(24) Hu, N.-H.; Norifusa, T.; Aoki, K. *Polyhedron* **1999**, *18*, 2987–2994.

Scheme 4. Routes from MT



Throughout this acidic region the data fit a line generated by eq 2.

$$k_{\text{obsd}} = \frac{K_{a1} \cdot K_{a2} \cdot k_2 + K_{a1} \cdot k_1 \cdot [\text{H}^+]}{K_{a1} \cdot K_{a2} + K_{a1} \cdot [\text{H}^+] + [\text{H}^+]^2} \quad (2)$$

The elimination of benzoylformate from MT is specific base-catalyzed

$$k_{\text{obsd}} = \frac{k_e \cdot [\text{OH}^-]}{K_w/K_{a3} + [\text{OH}^-]} \quad (3)$$

MT has three distinct protonation states, each with its own apparent rate of decarboxylation (Scheme 4). If the solution is more acidic than 0.03 M HCl, both the N1' and the carboxyl group are protonated. This form is unreactive. From 0.03 M to pH 4, only N1' of the pyrimidine is protonated, while the carboxyl is ionized. (The thiazolium is always positively charged due to its quaternary nitrogen center.) In this region decarboxylation is most rapid. From pH 4 to pH 8.5, N1' is not protonated and MT decarboxylates somewhat more slowly. The lower reactivity should reflect the reduced inductive effect that would stabilize the anionic portion of the transition state of the neutral pyrimidine. At higher pH, retrograde elimination of benzoylformate, followed by ring-opening of the resulting thiamin through addition of hydroxide, is the fastest process. This is described by eq 2, with  $[\text{OH}^-] \ll K_w/K_{a3}$ ,  $k_{\text{obsd}} = k[\text{OH}^-]$  (where  $k = k_e K_{a3}/K_w$ ). From fitting the observed rate constant to this equation,  $k_e$  for elimination is  $0.5 \text{ M}^{-1} \text{ s}^{-1}$ . We used data recorded at two wavelengths to deal with the base-catalyzed ring-opening reaction of the thiazolium group of thiamin.<sup>22</sup>

The apparent  $\text{p}K_a = 0.2$  (from  $K_{a1}$ ) that fits the data for the carboxyl group is very low but similar to other compounds of this type. The acid form overall is a dication due to the thiazolium and protonated pyrimidine. The second  $\text{p}K_a (= 3.9$  from  $K_{a2})$  is as expected for the conjugate acid of the pyrimidine.<sup>22</sup> The decarboxylation rate constants are  $(5.6 \pm 0.4) \times 10^{-4} \text{ s}^{-1}$  (low pH) and  $(3.0 \pm 0.4) \times 10^{-4} \text{ s}^{-1}$  (neutral solution), corresponding to the forms on either side of the  $\text{p}K_a$  of the pyrimidine.

As expected from the structure of MT and the likely transition state for decarboxylation, most buffers had no effect on the rate of the decarboxylation of MT. However, because the immediate product is subject to fragmentation, increasing concentrations of Brønsted acids, in general, divert the initial products formed upon loss of carbon dioxide from fragmentation (PTK and DMAP) to HBnT. Thus, protonation of the conjugate base of HBnT from the decarboxylation of MT is general acid catalyzed, consistent with the general base catalysis mechanism of C2 $\alpha$  deprotonation of HBnT. The effect of concentration of the acid component of the buffer on the product distribution gives information needed to calculate the specific rate constant for fragmentation and protonation based on the estimated  $\text{p}K_a$  for dissociation of the C2 $\alpha$  proton.

Thus, we did not expect the conjugate acid of pyridine, pyridinium, to accelerate decarboxylation of MT. There is no place in the structure of MT that would provide a place for addition of a proton from pyridinium prior to or during the step in which breaking of the carbon–carbon bond releases carbon dioxide, so the acid cannot lower the barrier for this process. Yet, the rate increases linearly with pyridinium concentration. In order to identify the source of the special acceleration



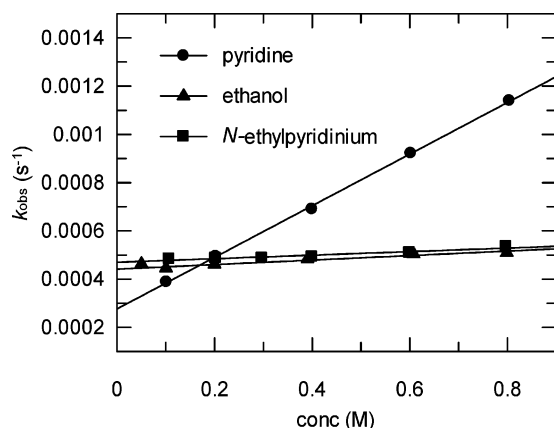


**Figure 2.** Observed first-order rate constants for decarboxylation of MT as a function of concentrations of pyridine, ethanol, and *N*-ethylpyridinium chloride in 0.2 M pyridine buffered solution at pH = p*K*<sub>a</sub>', *I* = 1.0, 25 °C. The second-order rate constants from the slopes of the plots: pyridine,  $k = (1.1 \pm 0.1) \times 10^{-3} \text{ M}^{-1} \text{ s}^{-1}$ ; ethanol,  $k = (9.3 \pm 1.2) \times 10^{-5} \text{ M}^{-1} \text{ s}^{-1}$ ; *N*-ethylpyridinium chloride,  $k = (7.3 \pm 1.1) \times 10^{-5} \text{ M}^{-1} \text{ s}^{-1}$ .

provided by pyridinium, we examined the effects of structurally related buffers on rate and product distribution. We also examined the effect on rate resulting from changing the dielectric of the medium by addition of ethanol to the same extent as from addition of pyridine, since the decarboxylation can be accelerated by transfer to organic solvents. The data in Figure 2 show that addition of pyridine accelerates the rate of the reaction in direct proportion to the concentration added. This apparent second-order process does not show saturation at accessible pyridine concentrations. Addition of ethanol, whose dielectric constant is close to that of pyridine, has very little effect.

In order to test further if the catalytic effects of pyridine are the result of the transfer of a proton or the result of electrostatic interactions, the effects of *N*-ethylpyridinium were assessed (Figure 2). The *N*-ethyl compound clearly has no significant effect, ruling out an electrostatic origin for the catalysis by pyridinium.

Apparent second-order rate constants obtained from the plots through the data in Figure 2 show that the effect of ethanol is less than 10% that of pyridine. The magnitude of the effect of ethanol indicates the extent that catalysis by pyridine could be due to its alteration of solvent polarity. This establishes that the effect of pyridine is not the result of its effect on the dielectric constant of the medium, a mechanism that has been widely proposed as a means of enhancing rates of thiamin catalysis.<sup>25–27</sup> If pyridine promotes decarboxylation through a mechanism mediated by solvent polarity, then addition of ethanol would have a large, additive contribution to the observed rate. Other additives have similar effects to that of ethanol with very small apparent rate constants: acetate ( $7.9 \times 10^{-5} \text{ M}^{-1} \text{ s}^{-1}$ ), phosphate ( $2.8 \times 10^{-5} \text{ M}^{-1} \text{ s}^{-1}$ ), and benzoate ( $9.9 \times 10^{-5} \text{ M}^{-1} \text{ s}^{-1}$ ) buffers.

Variation of the pyridine acid/base buffer ratio was used to determine the catalytically active component. The total concentration of buffer was less than 0.8 M. A plot of the second-order rate coefficient for decarboxylation of MT as a function

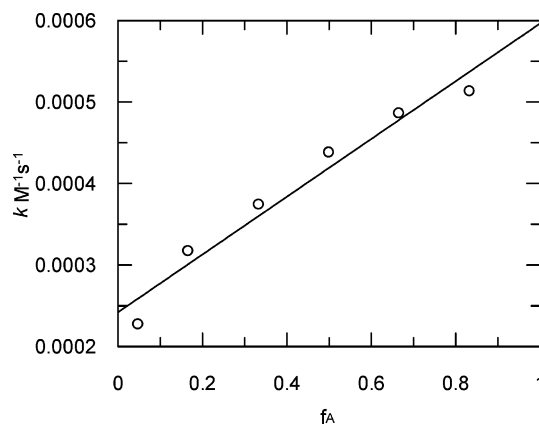


**Figure 3.** Second-order rate coefficient for decarboxylation of MT in pyridine buffer vs the acid fraction (*f*<sub>A</sub>) of the pyridine buffer (acid component/total buffer). pH = p*K*<sub>a</sub>', *I* = 1.0, 25 °C.

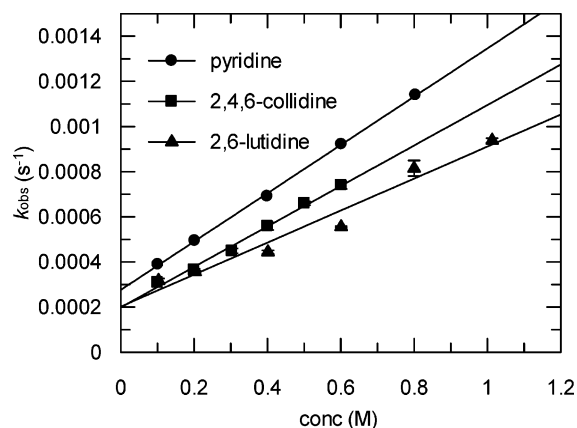


**Figure 4.** Dependence of the observed first-order rate constant for decarboxylation of MT on (substituted) pyridine buffer concentration. pH = p*K*<sub>a</sub>', *I* = 1.0, 25 °C.

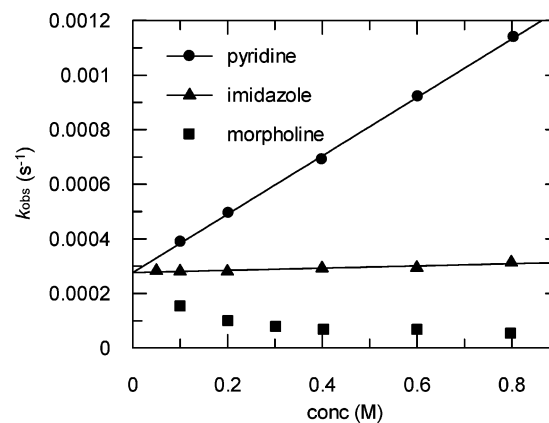


**Figure 5.** Contrasting dependence of the observed first-order rate constant on pyridine, imidazole, and morpholine buffer concentrations. pH = p*K*<sub>a</sub>', *I* = 1.0, 25 °C.

of the mole fraction of the acid component indicates that this is the catalytic component (Figure 3).

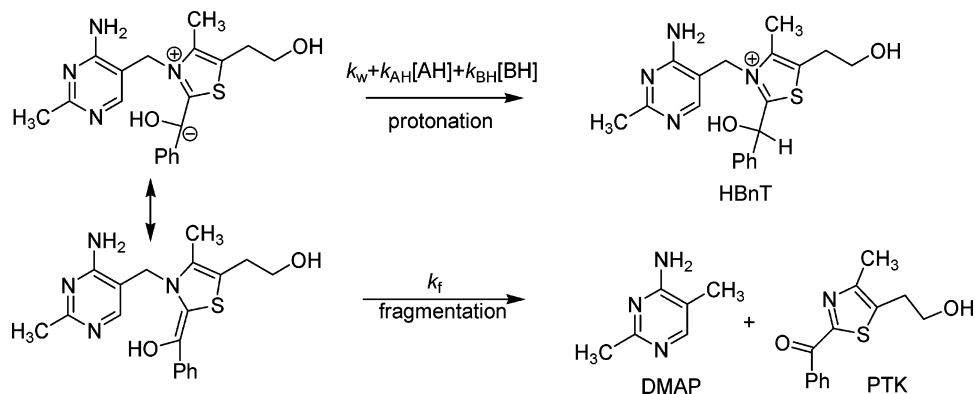
C-Alkyl pyridines (2,4,6-collidine, 2,6-lutidine, Figure 4) as well as 2-picoline and 4-picoline (not shown) are effective catalysts, but other nitrogen-containing heterocyclic bases are not effective, as exemplified by morpholine and imidazole (Figure 5).

**Product Distribution – Acid Catalyzed Formation of HBnT in Competition with Fragmentation.** The nonenzymic

(25) Crosby, J.; Stone, R.; Lienhard, G. E. *J. Am. Chem. Soc.* **1970**, 92, 2891–900.

(26) Gutowski, J. A.; Lienhard, G. E. *J. Biol. Chem.* **1976**, 251, 2863–2866.

(27) Kluger, R.; Gish, G.; Kauffman, G. *J. Biol. Chem.* **1984**, 259, 8960–5.

**Scheme 5.** Protonation vs Fragmentation

decarboxylation of MT gives the protonation product (HBnT) and fragmentation products (PTK and DMAP, Scheme 5).

Along with the conjugate acid of pyridine being able to promote decarboxylation far better than other types of acids, it is also a superior agent to transfer a proton and direct the product to HBnT. Thus, enhancing the rate of catalysis also directs the reaction away from fragmentation. This can explain the complete suppression of fragmentation in the enzymatic reaction as a direct consequence of its catalytic mechanism without additional assumptions. The rate of trapping cannot be measured directly since decarboxylation is the slower step, but the amount of HBnT formed as a function of acid concentration is an indicator of effectiveness in trapping; this can be directly related to the overall rate and efficiency of proton transfer. We compared the product distribution in the presence of pyridine with those resulting from the presence of acetate (pH 4.6), bis-tris (pH 6.7), 3,3,3-trifluoroethylamine (pH 5.7), and phosphate (pH 6.5). Because hydronium is also an effective acid catalyst for protonation to give HBnT, the lower the pH, the more protonation product, HBnT, is obtained relative to the fragmentation products. The protonation product fraction at zero buffer concentration from pH 4 to pH 7 is given in Figure 6. The zero-buffer curve is the fit of the data to eq 4 for trapping by hydronium ion:

$$\frac{\text{HBnT}}{\text{HBnT} + \text{PTK}} = \frac{k_w + k_{AH} * (10^{-\text{pH}})}{k_w + k_{AH} * (10^{-\text{pH}}) + k_f} \quad (4)$$

Here  $k_w$  is the rate constant for protonation by water,  $k_{AH}$  is the second-order rate constant for protonation by hydronium, and  $k_f$  is the rate constant for fragmentation. Fitting the data in Figure 6 to eq 4 gives  $k_w/k_f = 0.20 \pm 0.03$  and  $k_{AH}/k_f = 5.6 \pm 0.2 \times 10^4 \text{ M}^{-1}$ .

Formation of the C2 $\alpha$  conjugate base from HBnT is general base catalyzed. Therefore, protonation of the same conjugate base that is formed by decarboxylation of MT must be subject to general acid catalysis as a consequence of microscopic reversibility. The effect of added Brønsted acids on product distribution is shown in Figure 7 for imidazole and morpholine in competition with pyridine. The trapping of the enamine by Brønsted acids is subject to saturation as the route to the fragmentation products is overcome by the available acid; only HBnT forms at high buffer concentrations. The resulting fit of the data to a reversible binding equation yields a pseudoaffinity constant as the concentration needed to divert half the anion formed to HBnT. In each case, less pyridine is needed to achieve saturation.

C-Alkyl pyridines are the near equals of pyridine in catalyzing the decarboxylation, indicating that the association with MT is not subject to a significant steric effect. This is consistent with ring-stacking rather than perpendicular association. On the other hand, the data in Figure 8 show that 2,6-lutidine is about as effective as pyridine in trapping the conjugate base of HBnT, but 2,4,6-collidine is very ineffective although it is an effective catalyst for decarboxylation. This establishes that the mechanism that accelerates the decarboxylation need not be coincident with the trapping process.

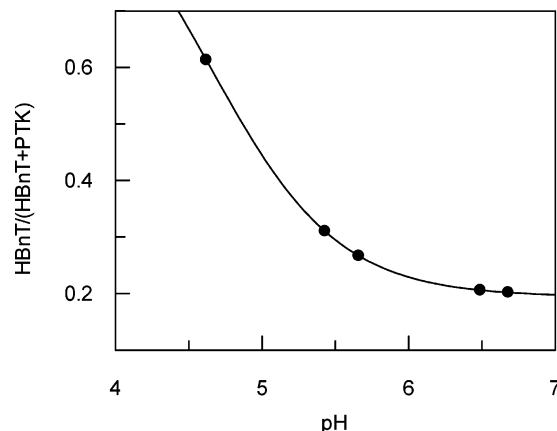


**Figure 6.** Fraction of HBnT formed from MT extrapolated to zero buffer concentration, pH 4 to pH 7. The line is a nonlinear regression fit to eq 4.  $I = 1.0$ , 25 °C.

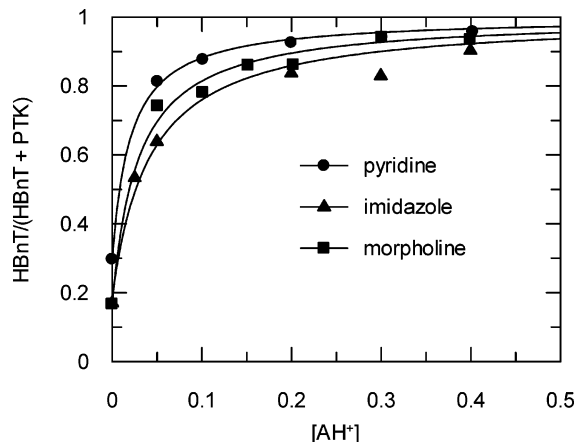


**Figure 7.** Effect of the acid component of pyridine, imidazole and morpholine buffers on product distribution from MT. pH = pK $_a'$ ,  $I = 1.0$ , 25 °C.

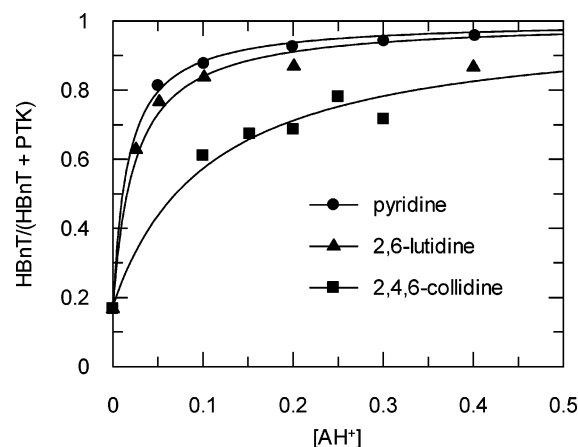


**Figure 8.** Dependence of product distribution on (substituted) pyridine concentration. pH =  $pK'_a$ ,  $I = 1.0$ , 25 °C.

**Internal Stacking Interactions.** We initiated calculation of the optimized structure of MT from the crystal structure of HBnT by substitution of a carboxyl group for the C2 $\alpha$  proton. The optimized structure shows  $\pi$ – $\pi$  stacking of the phenyl and pyrimidine rings. Such  $\pi$ – $\pi$  stacking exists in crystal structures of HBnT.<sup>24</sup> The association is likely to be weak since the observed catalysis by pyridinium does not show saturation at the moderate concentration levels in our studies.

## Discussion

In neutral solution, the conjugate of benzoylformate and thiamin, mandelylthiamin (MT), undergoes decarboxylation with a half-life at 25 °C of about 23 min; benzoylformate itself does not undergo any observable decarboxylation over long periods, even at higher temperature. When MTDP is isolated from a denatured mutant of indolepyruvate decarboxylase<sup>28</sup> that utilizes benzoylformate as a substrate, its decarboxylation rate constant ( $3.1 \times 10^{-4} \text{ s}^{-1}$  at 25 °C)<sup>6</sup> is identical to that reported here for decarboxylation of MT in neutral solution, confirming the validity of using MT as a reaction surrogate for MTDP. The carbanion resulting from loss of carbon dioxide from MT is readily delocalized, and the negative charge is cancelled by its internal positive charge. The stabilizing interactions are also likely to be present in the transition state leading to these products. Yet,  $k_{\text{cat}}$  of benzoylformate decarboxylase requires that the similar intermediate on the enzyme, MTDP, has a half-life that is only a fraction of a second. Thus, although conversion of benzoylformate to the conjugate of thiamin dramatically increases its reactivity, the enzyme is able to lower the barrier much further. Since BFD has several polar side chains in its active site,<sup>14,17</sup> desolvation of the substrate–TDP conjugate into a hydrophobic environment in order to provide catalysis would require an as yet unknown source for energy to achieve such a thermodynamically unfavorable extraction.

**Implying Pyridinium Catalysis by Association.** A key set of observations in the present study is that pyridinium and C-alkyl-pyridiniums increase the rate of decarboxylation of MT while other Brønsted acids do not. (The term “general acid catalysis” therefore does not rigorously apply. The term “specific acid catalysis” requires that only one species is active. Since a limited subset of Brønsted acids is catalytic, we could refer to

the kinetic effects of pyridinium and its derivatives as “selective acid catalysis”, a domain within Brønsted acid catalysis resulting from factors beyond the proton-transfer step itself.) We have also shown that catalysis by pyridine-derived acids is due to their proton-donating ability and not their solvent effect. However, the structure of MT presents no opportunity for addition of a proton during the decarboxylation step. The calculated structure of MT shows that phenyl and pyrimidine rings are associated face-to-face. Based on this model, we assume that pyridines can also associate with the phenyl group. C-Alkylation of pyridine should not interfere with this interaction. Therefore, pyridines can associate with MT prior to the cleavage that leads to formation of carbon dioxide (Scheme 6, reaction A). For simplicity we show pyridine as its conjugate acid only. In the absence of pyridine, reversal addition of the enamine to carbon dioxide occurs readily (Scheme 6, Reaction B). Theoretical analysis of decarboxylation reactions indicates that there is a very low barrier for addition to the acceptor of carbon dioxide when the components are in close proximity.<sup>29–32</sup>

Venkatasubban and Schowen observed situations in which an acid catalyst necessarily associates with the subject of catalysis in advance of a proton transfer.<sup>33</sup> They named this metaphorically: “spectator catalysis.” Jencks cited similar association reaction patterns,<sup>34</sup> coining the more widely used term “preassociation mechanism.” Applying these ideas, we see that Brønsted acid catalysts will only be effective in promoting decarboxylation if the acid associates with the reactant prior to the decarboxylation step. This also predicts that acids that are not spectators will be unable to compete at this stage due to their need to diffuse to the reaction site. The barrier to separation of carbon dioxide from the enamine (the major resonance contributor of the residual carbanion) is higher than the barrier to reaction with the enamine. This makes the rate-determining step in the decarboxylation of MT the separation of carbon dioxide from the enamine. Prior protonation of the enamine provides a competing mechanism in which separation of carbon dioxide is no longer kinetically significant.

Another important aspect of reactivity of the enamine is the competition of protonation to give HBnT with the rapid fragmentation of the unprotonated form. Pyridine acids should be more effective at lower concentrations than other acids in diverting the process from fragmentation to formation of the expected product, HBnT, as we observe. An overall scheme that accommodates our results is shown in Scheme 7. The competition among steps associated with  $k_1$ ,  $k_{-1}$ ,  $k_2$ , and  $k_3$  controls the overall rate and product distribution.

An acid associated with MT prior to decarboxylation can provide catalysis whereas one that is not associated with MT prior to the reaction could not arrive in time to be of any effect. Complex formation prior to carbon–carbon bond-breaking would permit efficient protonation at C2 $\alpha$ , accelerating the net forward rate of the reaction by quenching the reactive species.

In our studies, the association of pyridinium and MT is not complete; the observed catalysis remains second-order without

(29) Acevedo, O.; Jorgensen, W. L. *J. Org. Chem.* **2006**, *71*, 4896–4902.

(30) Gao, J.; Byun, K. L.; Kluger, R. *Top. Curr. Chem.* **2004**, *238*, 113–136.

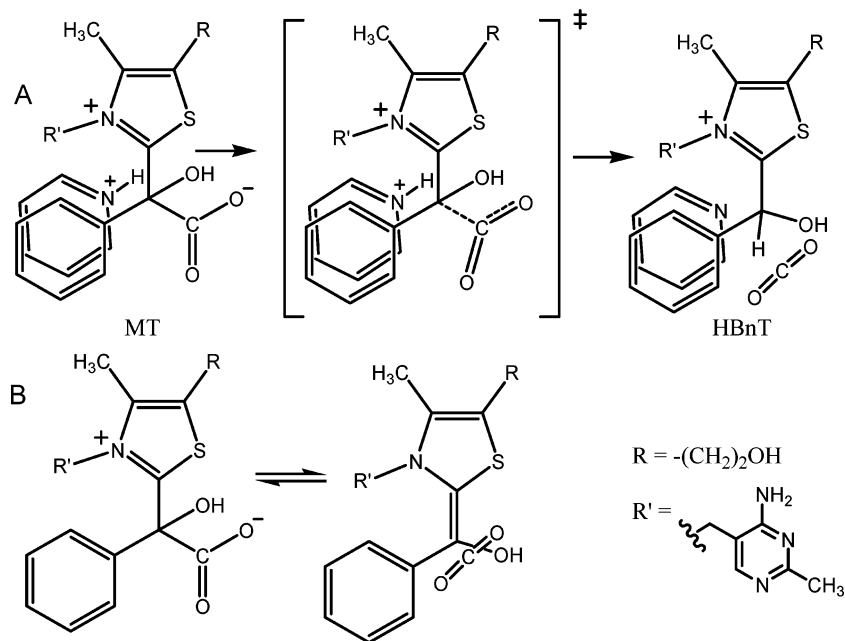
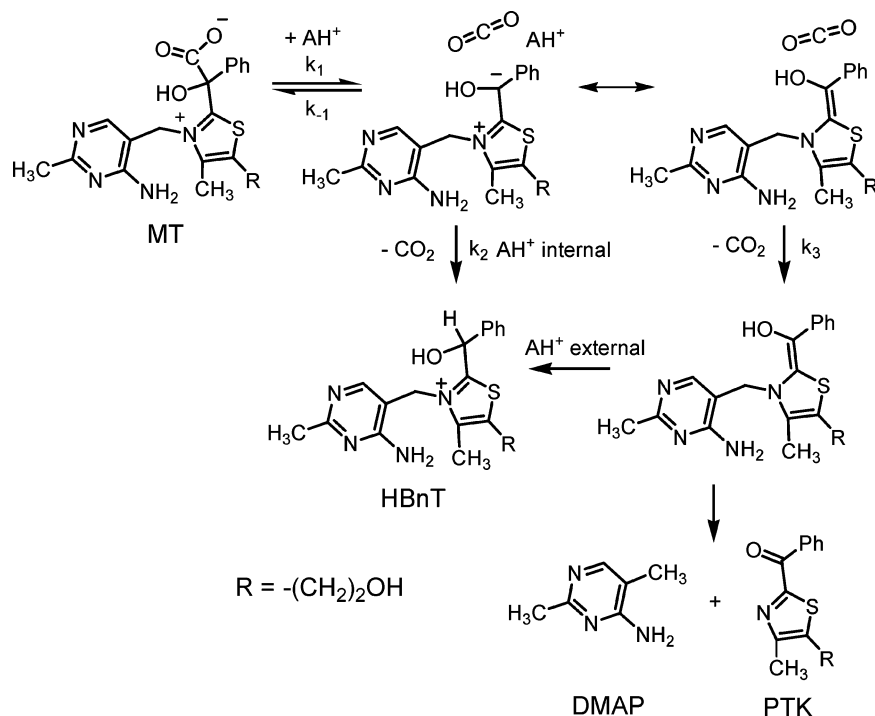
(31) Gao, J.; Ma, S.; Major, D. T.; Nam, K.; Pu, J.; Truhlar, D. G. *Chem. Rev.* **2006**, *106*, 3188–209.

(32) Wu, N.; Mo, Y.; Gao, J.; Pai, E. F. *Proc. Natl. Acad. Sci. U.S.A.* **2000**, *97*, 2017–22.

(33) Venkatasubban, K. S.; Schowen, R. L. *J. Org. Chem.* **1984**, *49*, 653–655.

(34) Jencks, W. P. *Acc. Chem. Res.* **1976**, *9*, 425–432.

(28) Schütz, A.; Sandalova, T.; Ricagno, S.; Hübner, G.; König, S.; Schneider, G. *Eur. J. Biochem.* **2003**, *270*, 2312–2321.

**Scheme 6.** Selective Acid Catalysis via  $\pi$ -Stacking of Pyridinium and Phenyl Moieties**Scheme 7.** Competing Pathways Involving  $CO_2$  Separation and Selective Acid Catalysis

achieving even partial saturation. Thus, we can neither separate rates of association and proton transfer nor detect a complex spectroscopically. However, the failure of other acids to produce similar effects, while pyridinium and C-alkyl pyridiniums are effective, implicates a selective interaction based on structure rather than acidity. Furthermore, the lack of effect of *N*-ethylpyridinium shows that catalysis is not the result of electrostatic stabilization of the transition state.

**Acid Catalyzed Decarboxylation in TDP Enzymes.** The active site of BFD has two histidines with side chains that can serve as Brønsted acids. Mutation of one of the histidines to a nonacidic group reduces  $k_{cat}$  of the overall reaction to a level that is about the same as the reactivity of MT.<sup>17</sup> In the protein,

association of the acid and the intermediate does not depend on incidental stacking because the active site can provide specific interactions determined by spatial arrangements. Thus, we propose that for a decarboxylase in which a proton is transferred to an acceptor (to generate the precursor of an aldehyde), Brønsted acid catalysis will promote the reaction while avoiding fragmentation reactions resulting from the enamine, an effect that could also occur in a low polarity site.<sup>35</sup> This also provides a basis for the observation that although nonenzymic fragmentation of the enamine derived from MTDP is faster than the normal enzymic reaction of MTDP,<sup>18</sup> pro-

(35) Zhang, S.; Liu, M.; Yan, Y.; Zhang, Z.; Jordan, F. J. *Biol. Chem.* **2004**, 279, 54312–54318.



tonation of the conjugate base of HBnTDP that accelerates departure of CO<sub>2</sub> also blocks fragmentation by conversion of the enamine to HBnTDP.

In TDP-dependent decarboxylases where the ultimate product is not an aldehyde, protonation is counterproductive, ultimately requiring deprotonation. This is not a problem in terms of catalytic mechanisms. The immediate product of decarboxylation can be oxidized or it may react as a nucleophile toward an electrophilic partner in competition with trapping of nascent carbon dioxide. In all these processes, which are Lewis acid–base combinations, the second reactant may be bound prior to the decarboxylation step and therefore can undergo its reaction prior to separation of carbon dioxide. In those cases, a polar active site is also not necessary.<sup>36,37</sup>

**Decarboxylation vs Deprotonation.** Normally, decarboxylation is part of an electrophilic substitution process where carbon dioxide is replaced by a proton. The cleavage of the carbon–carbon bond and departure of carbon dioxide must precede protonation of the intermediate anion. For comparison, in an electrophilic substitution involving proton removal and addition exclusively, a base receives the proton and will be present in the transition state. Increased concentrations of Brønsted bases linearly increase the rate of the reaction. Unlike proton transfer, decarboxylation in water would normally not be promoted by an added catalyst, as the breaking of the carbon–carbon bond occurs without transfer to an acceptor: carbon dioxide forms from the elements of the carboxylate group. In the special case provided by MT, we see what initially appears to be paradoxical catalysis by a Brønsted acid with a leaving group that is an electrophile. We are conditioned to expect an acceptor of the leaving group to facilitate the process. Instead, the acid provides a means of interjecting a proton between carbon dioxide and the residual carbanion, a very unusual circumstance but very reasonable within the terms of the detailed mechanism and one that is consistent with enzymes where association occurs inherently.

**Carboxylation.** Carboxylase enzymes, which replace a proton with a carboxylate derived from bicarbonate, may take advan-

tage of the tendency of associated carbon dioxide to add readily to a nearby carbanion. The pioneering study of carbonate monoesters by Sauers, Jencks, and Groh<sup>38</sup> provides a general scheme for such a process. Carbon dioxide is generated near the acceptor by ATP-promoted dehydration of bicarbonate. The carbon dioxide is a much better electrophile than bicarbonate and would readily be trapped by a carbanion. The authors propose that the role of ATP in biotin-dependent carboxylases is to provide the driving force to dehydrate bicarbonate at an active site. Recent theoretical analysis of the decarboxylation reaction of a model of carboxybiotin shows that formation of carbon dioxide occurs prior to its solvation.<sup>29</sup> The use of carbon dioxide addition to carbanions in synthesis is consistent with such a reactivity pattern as well.

**Extensions.** The accessibility of the selective acid catalysis mechanism for decarboxylation reactions provides an opportunity to consider in detail some of the more general aspects of enzyme catalysis and interpret previously reported results. For example, <sup>12</sup>C/<sup>13</sup>C isotope effects in nonenzymic decarboxylation reactions are used to calculate an intrinsic barrier for comparison to enzyme catalyzed decarboxylation. This assumes that the isotope-sensitive step in the nonenzymic reaction occurs without any reversible component—that it is fully committed. It may well be that the enzymatic reactions are faster because they are more effectively unidirectional and the intrinsic isotope effect in the nonenzymic reaction is masked by a lack of commitment.

In summary, our studies indicate that decarboxylation can be catalyzed by a spectator or preassociated catalyst. This provides a consistent explanation for the additional acceleration of decarboxylation seen in enzymes that generate aldehyde precursors from derivatives of TDP while avoiding rapid side reactions. This can be generalized to other modes of trapping carbanions that result from formation of carbon dioxide.

**Acknowledgment.** We thank NSERC Canada for support through a Discovery Grant. Professors James C. Fishbein, J. Peter Guthrie, and John P. Richard provided insightful comments during the course of this work.

JA066249J

(36) Mansoorabadi, S. O.; Seravalli, J.; Furdul, C.; Krymov, V.; Gerfen, G. J.; Begley, T. P.; Melnick, J.; Ragsdale, S. W.; Reed, G. H. *Biochemistry* **2006**, *45*, 7122–7131.

(37) Frank, R. A. W.; Titman, C. M.; Pratap, J. V.; Luisi, B. F.; Perham, R. N. *Science* **2004**, *306*, 872–876.

(38) Sauers, C. K.; Jencks, W. P.; Groh, S. *J. Am. Chem. Soc.* **1975**, *97*, 5546–5553.